Desalination and Water Treatment
www.deswater.com
doi: 10.1080/19443994.2013.795255

51 (2013) 4907–4913
July

Taylor & Francis
Taylor & Francis Group

Pressure fields in an industrial UF module: effect of backwash

G. Cano[a], P. Steinle[a], J.V. Daurelle[b], Y. Wyart[a], K. Glucina[c], D. Bourdiol[d], P. Moulin[a,*]

[a]*Laboratoire de Mécanique, Modélisation et Procédés Propres (M2P2-CNRS-UMR 7340), Université Paul Cézanne Aix Marseille, Europôle de l'Arbois, BP 80, Bat. Laennec, Hall C, 13545 Aix en Provence cedex 04, France Tel. +33 6 67 14 14 18; Fax: +33 4 42 90 85 15; email: philippe.moulin@univ-amu.fr*
[b]*Institut Universitaire des Systèmes Thermiques Industriels (IUSTI-CNRS-UMR 6595), Aix-Marseille Université Technopôle de Château-Gombert, 5 rue Enrico Fermi, 13453 Marseille cedex 13, France*
[c]*Suez Environnement, CIRSEE, Pôle Qualité Eau, 38, rue du Président-Wilson, 78230 Le Pecq, France*
[d]*Degremont Technologie, Aquasource, 20 avenue Didier Daurat 31029 Toulouse cedex, France*

Received 3 September 2012; Accepted 17 February 2013

ABSTRACT

In the last decade, membrane manufacturers have improved their ultrafiltration module to raise the production of drinking water in order to meet an increasing demand. The usual process used is an inside-out filtration in dead-end mode. In this configuration, the energy consumption is limited by outside-in backwashes. Raising the permeability of the membranes lead to an increase in module compactness and strongly modify the driving force in the module. This study presents a computational fluid dynamics (CFD) model to predict the pressure and velocity field in the hollow fiber network (HFN) taking into account several parameters as the geometry of the module, the inlet pressure, gravity, and temperature. For the industrial tested module configuration, results shown that hollow fibers work in a homogeneous way in filtration mode but a great heterogeneity appear during the backwash. All the results have been validated compared with experimental values.

Keywords: Ultrafiltration; Hollow fiber module; Pressure and velocity fields; Backwash

1. Introduction

The ultrafiltration process in drinking water production is part of a growing industry, especially for the investigated waste water treatment process. The membrane manufacturers have improved membranes by increasing their permeability and developed modules with higher specific surfaces: the configuration generally used is an inside-out filtration in dead-end mode in order to minimize the energy consumption. By increasing the filtration surface and the membrane permeability, the permeate flow raises that leads to increase the module compactness and strongly modifies the module hydrodynamics [1,2]. It is then important to verify whether all the hollow fibers are subjected to the same pressure field as the transmembrane pressure (TMP). From the conception of the first hollow fiber modules, studies showed that one of the factors which limit the flow, besides fouling, was the pressure drop in the hollow fiber network (HFN), reducing the driving force

*Corresponding author.

Presented at the Conference on Membranes in Drinking and Industrial Water Production. Leeuwarden, The Netherlands, 10–12 September 2012. Organized by the European Desalination Society and Wetsus Centre for Sustainable Water Technology

and also the compaction which has a direct impact on the permeate flow as it increases the resistance to mass transfer [3]. In the case of heterogeneity of the pressure field, filtration and thus fouling are modified, but also the efficiency of the backwash, which is also a function of this pressure field in outside-in filtration. Many approaches by numerical simulation [4,5] or by models have tried to predict these performance changes. Mendret et al. [6] have shown the effect of nonuniform membrane permeability on the deposit construction in dead-end ultrafiltration by numerical investigation and its consequences on the filtration velocity profile along the membrane. Serra et al. [7,8] modeled the filtration and backwashing in hollow fiber modules. It was clearly demonstrated that there is an optimum value for the fiber diameter and for the void fraction, which is a compromise between the increase of the filtrating surface and the pressure drop.

This study proposes to determine by numerical simulation the pressure and velocity fields in a hollow fiber ultrafiltration module for the drinking water production process. The configuration used is an inside-out filtration in dead-end mode. If increasing the membranes permeability and filtration surface leads to an increase in the permeate flow, then the membrane packing density increases and strongly modify the hydrodynamic behavior of the module. It is then important to know whether all the fibers are subjected to the same pressure field as the TMP taking into account the exact geometry of the module, the membrane's permeability, the number of fibers in the module and the distance between each fiber.

2. Materials and methods

The investigated membrane module from Aquasource is worked in an inside-out filtration in dead-end mode. This study concerns the AC1125 Module. The hollow fibers have an internal diameter of 0.93 mm and an outer diameter of 1.66 mm (MWCO = 80 kDa). The geometry of the UF module used in this study presents 8 identical sections containing 4,500 hollow fibers each spaced by grids allowing a good distribution of the fluid around the membranes. The form and distribution of the holes on the central pipe allow the production of permeate during the filtration mode and the injection of clean water during the backwash.

2.1. Numerical model

The CFD model is developed using STARCCM+. Hollow fibers detailed geometry cannot be modeled due to the calculation time and memory needed, thus the membrane area is modelized as an orthotropic porous medium, where Darcy law governs fluid flow with a directional permeability tensor k. The latter depends on the arrangement of the fibers and the apparent porosity. Microscopic simulations at the hollow fibers scale have been carried out for two different arrangements in order to determine the permeability as a function of porosity. Once the tensor evaluated, macroscopic simulations are performed at the macroscopic scale. Two different zones appear in the whole module and each one is governed by a different flow model. In the hollow fibers zone, the Darcy model is solved. In the rest of the module the Navier–Stokes equation is applied. Into the central pipe and injection nozzles, the Reynolds number can reach 250,000 and require a turbulent model: the RANS « K–ε Realizable » is used. A laminar model is applied where Reynolds number is under 2,500.

2.2. Evaluation of the permeability K tensor

We determine the permeability tensor for the three directions $\overline{XX}$, $\overline{YY}$, and $\overline{ZZ}$ taking into account the two different distribution of the hollow fibers (in line and staggered arrangement) proposed by Brinkert et al. [9] (Fig. 1).

The permeability in the direction parallel $\overline{ZZ}$ to the fiber is given using the concept of hydraulic diameter and the Hagen–Poiseuille velocity in straight conduits Happel and Brenner [10]. The permeability in the direction parallel to the fibers is much higher compared with transversal's, its influence on pressure and velocity field in the module will be low.

To calculate, the transversal permeability constant K in the directions of $\overline{XX}$ and $\overline{YY}$, simulations have been performed on microscopic scale for the two different arrangements as well as for porosities ranging from the minimal to the maximum values. These simulations cover an elementary pattern of the HFN, describing the membrane including the membrane support as a homogeneous and isotropic porous media. The resistance of this porous media has been calculated under the assumption of laminar flow through the membrane, which means the flow rate is proportional to the TMP. Fig. 2 explains the used geometry set up and shows the resulting pressure and velocity fields for one of the simulations.

After that the mesh has been refined several times, the optimized mesh is obtained and the result is shown in Fig. 3 including the pressure profile in the membrane. The screenshots on the right side show the difference between a mesh (top) and the optimized mesh (bottom) on the boundary of the porous body.

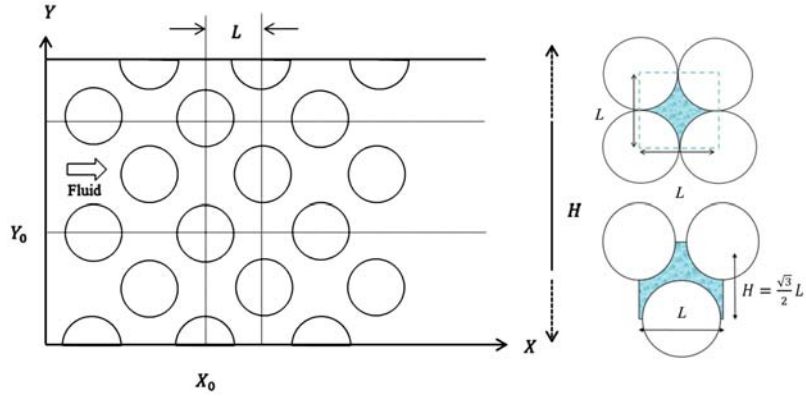

Fig. 1. Fluid flow across a bank of cylinders and possible cylinder arrangements (top right: inline and bottom right: staggered).

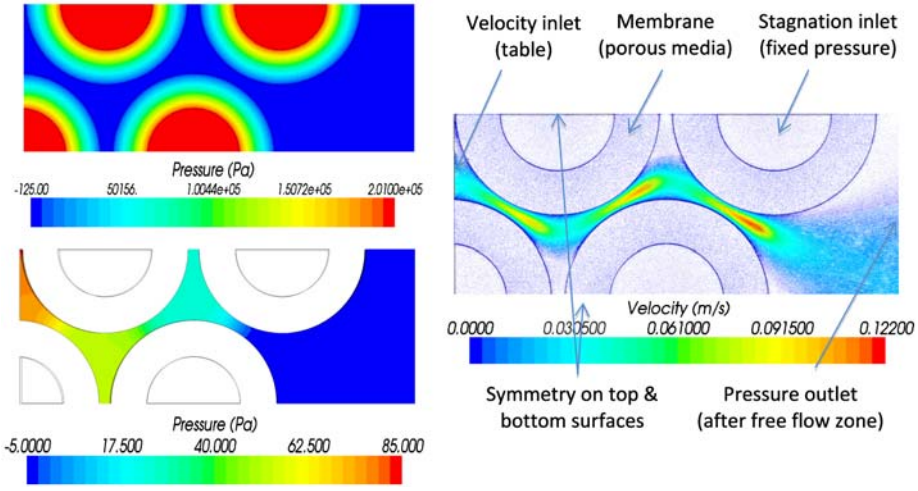

Fig. 2. Geometry, pressure field, and velocity vectors in an elementary pattern of the HFN. (Staggered arrangement; porosity $\varepsilon = 0.2$; TMP = 2 bar).

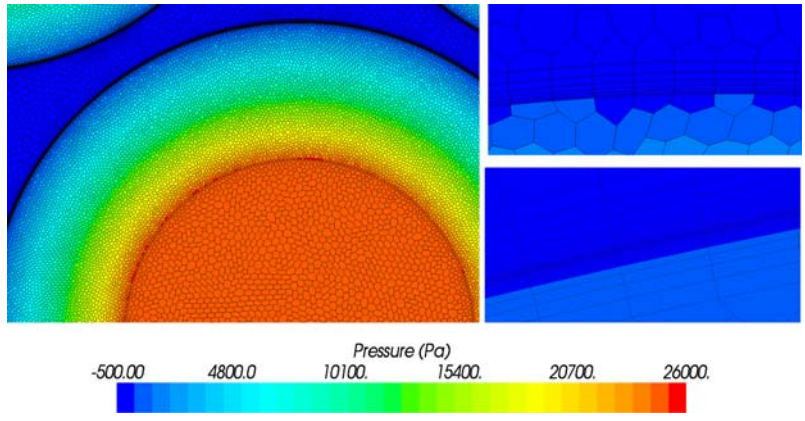

Fig. 3. Pressure field in the membrane (left), mesh on the boundary to the porous body (top right) and the refined mesh with a very fine prism layer on the boundary to the porous (bottom right). (Staggered arrangement; porosity $\varepsilon = 0.2$; TMP = 0.25 bar; filtration mode).

In the end, a very fine prism layer structure in combination with a refinement in the porous body as well as in the gaps gave the best results. The overall mesh contained about two million cells, with a very high compaction of cells in the porous and on the boundary layers between the interfaces. Additional, to a volumetric control of the cell size in the porous body, eight prism layers have been used on both sides of the interface.

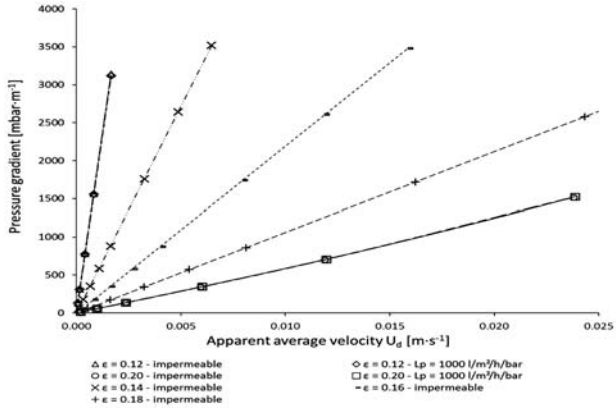

Fig. 4. Comparison of the pressure drop across the bundle of hollow fibers with permeable and impermeable walls for different porosities and both as a function of the transverse velocity. (Staggered arrangement; TMP = 0.25 bar).

To cover the periodicity, the velocity inlet has been performed with a table, which allows us to impose a fully developed flow in the entrance section. Additional, mass flow is entering the system from the inner side of the hollow fibers by imposing a pressure difference with a stagnation inlet inside the fiber and a pressure outlet on the right. The top and bottom surfaces are defined as symmetry planes and the cut has been chosen very thin, to maximize the mesh quality. These simulations were used to plot the pressure gradient as a function of the apparent average velocity crossing the fibers and they were compared with simulations of the HFN with impermeable walls (Fig. 4).

As the permeation represents less than 1% on the pressure drop, the hollow fiber can be considered as a solid wall in the further simulations.

The curves describing the permeability as a function of porosity for both configurations follow similar polynomial law (Fig. 5). This permeability tends towards 0 for low porosities which means that the resistance (viscous) tends towards infinity in the solid matrix.

Arrangement	Range of porosity	Equation
In line	0.22 – 0.3	$y = 2E\text{-}07x^3 - 1E\text{-}07x^2 + 2E\text{-}08x - 1E\text{-}09$
Staggered	0.1 – 0.2	$y = 9E\text{-}08x^3 - 2E\text{-}08x^2 + 2E\text{-}09x - 6E\text{-}11$

Example for the staggered arrangement

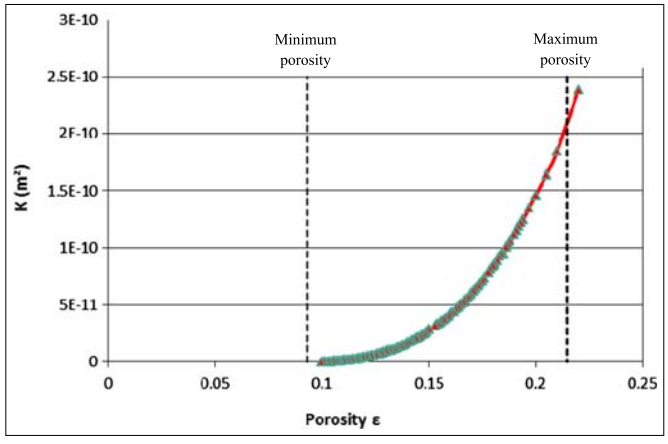

Fig. 5. Variation of the permeability K (m^2) as a function of a wide range the porosity ε for an in-line and a staggered arrangement of the hollow fibers.

3. Results

3.1. Evaluation of pressure field in the module

The Navier–Stokes equations in the module have been performed considering the different parameters as the geometry of the module and membranes, the hydraulic permeability of the membrane L_p and their compactness, the operating entry values such as filtration or backwash pressures, gravity, and temperature. In the case, of filtration hollow-fibers work in an homogeneous way (+/− 0.4%) with a very low compacity all over the module.

However, during the backwash, a greater heterogeneity may appear. Hollow-fibers are subjected to a pressure and the fluid motion tends to compact the hollow-fibers together. This compaction is not homogeneous along the length because of the potting at each extremity of the module. For this part of the study the arrangement effect, the variation of the permeability and the pressure, the arrangement effect and the influence of porosity, temperature and gravity was taken into account. For realistic case of backwash we can estimate the flow losses of the entire module: considering a hydraulic permeability of 200 L h^{-1} bar^{-1} m^{-2}, an inlet pressure of 2 bars, the module AC1125 developing 125 m^2 of membrane surface, a porosity of 0.12, the theoretical flow is 50 m^3 h^{-1}. Results of simulation give a pressure drop between the center and the edge of the bundle of around 200 mbar and represent a loss of 10% of the total flow caused by the heterogeneity of the pressure within the bundle (Fig. 6).

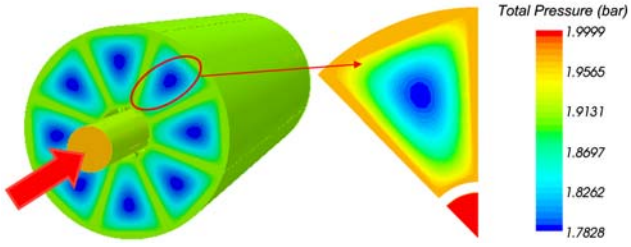

Fig. 6. Pressure field (AC1125 Backwash mode out-in, Inlet Pressure $P_i = 2$ bar; $T = 25$ °C, $\varepsilon = 0.12$).

For a high values of the inlet pressure and membrane permeability, respectively 2 bars and 1,000 L h^{-1} bar^{-1} m^{-2}, whatever the HFN porosity, and due to the passage of fluid in the central pipe nozzle that distributes the permeate within the module to perform the backwash, the pressure strongly decrease (15%) and 1.7 bars is obtained around the HFN. Pressure is identical and homogeneous around the bundle of hollow fibers. For a porosity of 0.12, the range of pressure inside the HFN is 1.7–1 bar. In this limit case, the hollow fibers from the edge are washed with a TMP of around 1.7 bar whereas fibers from the center backwash are washed with a TMP of 1.1 bar: the loss of flow due to the pressure drop is equal to 32% (Fig. 7).

3.2. Experimental validation

The validation of the CFD results was performed using the AC1125 UF module from the company

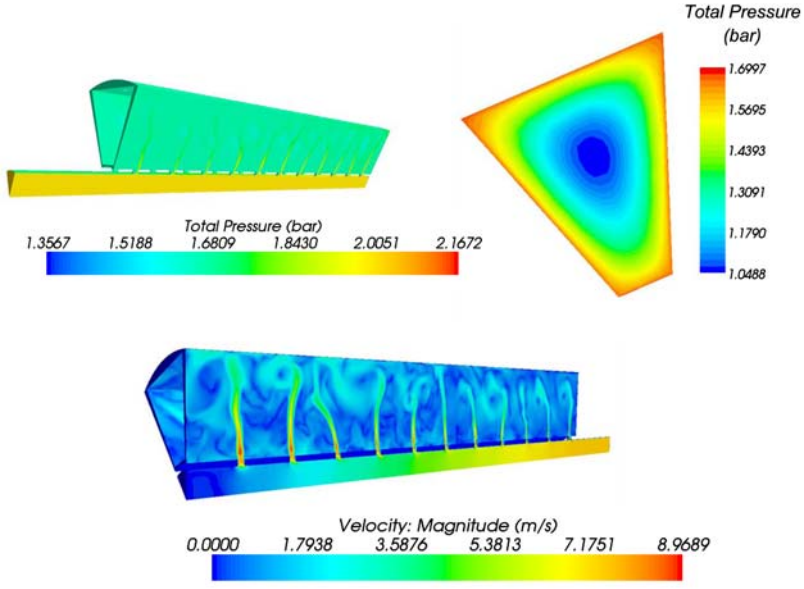

Fig. 7. Pressure (top) and velocity (bottom) fields (AC1125 backwash mode out-in, Inlet Pressure $Pi = 2$ bar; $T = 25$ °C, $\varepsilon = 0.12$) for a high permeability of 1,000 L h^{-1} bar^{-1} m^{-2}.

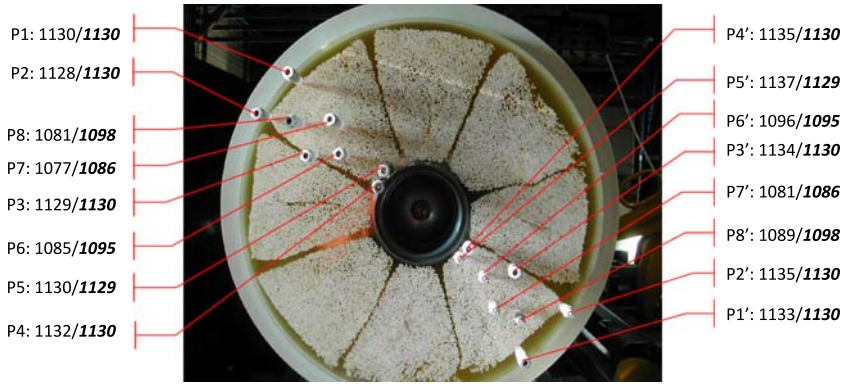

Fig. 8. Experimental pressure measurement in the hollow fiber bundle compared with values obtained by numerical simulations in mbar—(experiment/simulation)—(AC1125 backwash mode out-in, inlet pressure $Pi = 2$ bar; $T = 26$ °C; $\varepsilon = 0.14$).

Aquasource that is equipped with two packs of eight pressure sensors as shown in Fig. 8. Five of them are placed on the periphery of the module while the others are inside the HFN. In order to measure the hydraulic pressure, the fibers concerned are blocked at one end and a connector is glued to the other side to connect it to a pressure sensor and act as a static pressure. For a temperature of 26 °C, the pressure sensors positioned at the periphery of the HFN give a constant pressure while the other give a lower pressure as expected. The results between experiments and numerical simulation are matching and the found value of the HFN porosity is to 0.14. For this industrial module, a variation of the temperature between 12 and 26 °C provides a pressure difference between the outside and the center of the HFN, respectively from 31 to 53 mbar. The numerical simulation gives respective values of 33 and 47 mbar. This good agreement lead us to validate the numerical model which allow to predict the pressure field in the HFN whatever the parameters.

4. Conclusion

We have shown that during inside-out filtration and for the three tested module configurations and even for unrealistic conditions of filtration (for example inlet pressure of 2 bars), hollow-fibers work in an homogeneous way +/− 0.4%.

However, in the case of the backwash, a greater heterogeneity may appear. This latter is especially dependent on the porosity of the hollow-fiber bundle which tends to be low because of the compaction of the hollow-fibers subjected to a high pressure in that direction. The pressure difference within the bundle appears logical between the edge and the center of the bundle. This difference is due to the loss of pressure in the bundle, but also the loss of matter caused by the permeation of the hollow-fibers. The effect of gravity is a classic linear effect that can be taken into account. For a given permeability and porosity, it appears that the pressure of the inlet backwash increases and the pressure difference between the edge and the center of the bundle increases. Relatively, the ratio pressure difference on inlet pressure remains constant. For a given permeability and inlet pressure, the effect of the porosity on the filtration's homogeneity is as high as the latter is low: a polynomial variation is obtained. For a constant product permeability inlet pressure, the heterogeneity will be as strong as the permeability is high. This proves, in a practical manner that it is not reasonable for a given module's geometry to replace hollow-fibers by more permeable hollow-fibers without lowering the efficiency of the backwash. In post treatment, it is therefore possible to calculate the global flow produced by the module and to estimate comparing with a theoretical value equal to the product surface permeability inlet pressure the loss of flow caused by the heterogeneity of the pressure within the bundle. For some conditions, the overall flow loss can reach 32%. Obviously, these numerical simulations have been validated by experimental measurements.

Acknowledgments

The CFD computations were performed using STARCCM+ code from CD-ADAPCO.

References

[1] J. Zheng, Y. Xu, Z. Xu, Flow distribution in a randomly packed hollow fiber membrane module, J. Membr. Sci. 211 (2003) 263–269.

[2] S. Chang, T. Fane, The effect of fibre diameter on filtration and flux distribution-relevance to submerged hollow fibers module, J. Membr. Sci. 184 (2001) 221–231.
[3] K.M. Persson, V. Gekas, G. Trägårdh, Study of membrane compaction and its influence on ultrafiltration water permeability, J. Membr. Sci. 100 (1995) 155–162.
[4] R. Ghidossi, D. Veyret, P. Moulin, Computational fluid dynamics applied to membranes: State of art and opportunities, Chem. Eng. Proc. 45 (2006) 437–454.
[5] R. Ghidossi, J.V. Daurelle, D. Veyret, P. Moulin, Simplified CFD approach of a hollow fiber ultrafiltration system, Chem. Eng. J. 123 (2006) 117–125.
[6] J. Mendret, C. Guigui, C. Cabassud, P. Schmitz, Numerical investigations of the effect of non-uniform membrane permeability on deposit formation and filtration process, Desalination 263 (2010) 122–132.
[7] C. Serra, M.J. Clifton, P. Moulin, J.C. Rouch, P. Aptel, Dead-end ultrafiltration in hollow fiber modules: Module design and process simulation, J. Membr. Sci. 145 (1998) 159–172.
[8] C. Serra, L. Durand-Bourlier, M.J. Clifton, P. Moulin, J.C. Rouch, P. Aptel, Use of air-sparging to improve backwash efficiency in hollow-fiber modules, J. Membr. Sci. 161 (1999) 95–114.
[9] L. Brinkert, P. Paris, M. Renner, J.M. Espenan, P. Aptel, Pressure drops in radial flow membrane modules for ultrafiltration hollow fibers, J. Membr. Sci. 92 (1994) 131–139.
[10] J. Happel, H. Brenner, Low Reynolds Number Hydrodynamics: With Special Applications to Particulate Media (Mechanics of Fluids and Transport Processes), Matinus Nijhoff Publishers, The Hague, 1983, ISBN: 10:9024728770.